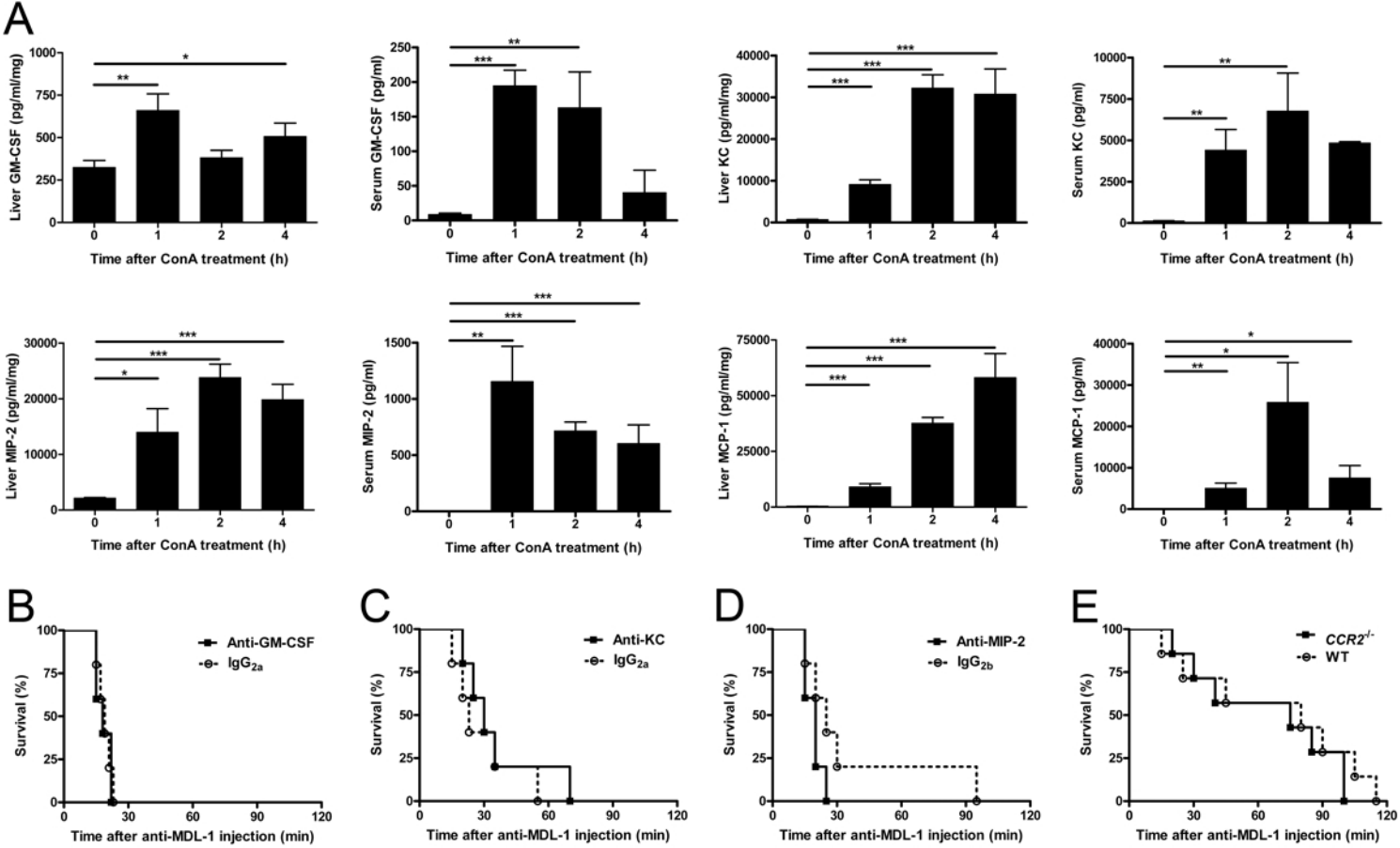

Supplemental Figure 1. ConA increased GM-CSF, KC, MIP-2 and MCP-1 production but they are not involved in MDL-1-triggered shock. **(A)** Liver homogenates and sera were obtained from mice treated with ConA for indicated times (n=5). GM-CSF, KC, MIP-2 and MCP-1 levels in liver homogenates and sera were quantitated by Luminex. *P<0.05, **P<0.01, ***P<0.001 compared to 0 h time point. **(B-D)** Mice were pretreated with anti-mouse neutralizing mAbs for **(B)** GM-CSF, **(C)** KC, **(D)** MIP-2 and corresponding isotype control (n=5) prior to administration of ConA followed by anti-MDL-1 mAb, and survival was monitored. **(E)** *CCR2*$^{-/-}$ and WT mice (n=5) were treated with ConA followed by anti-MDL-1 mAb, and survival was monitored.

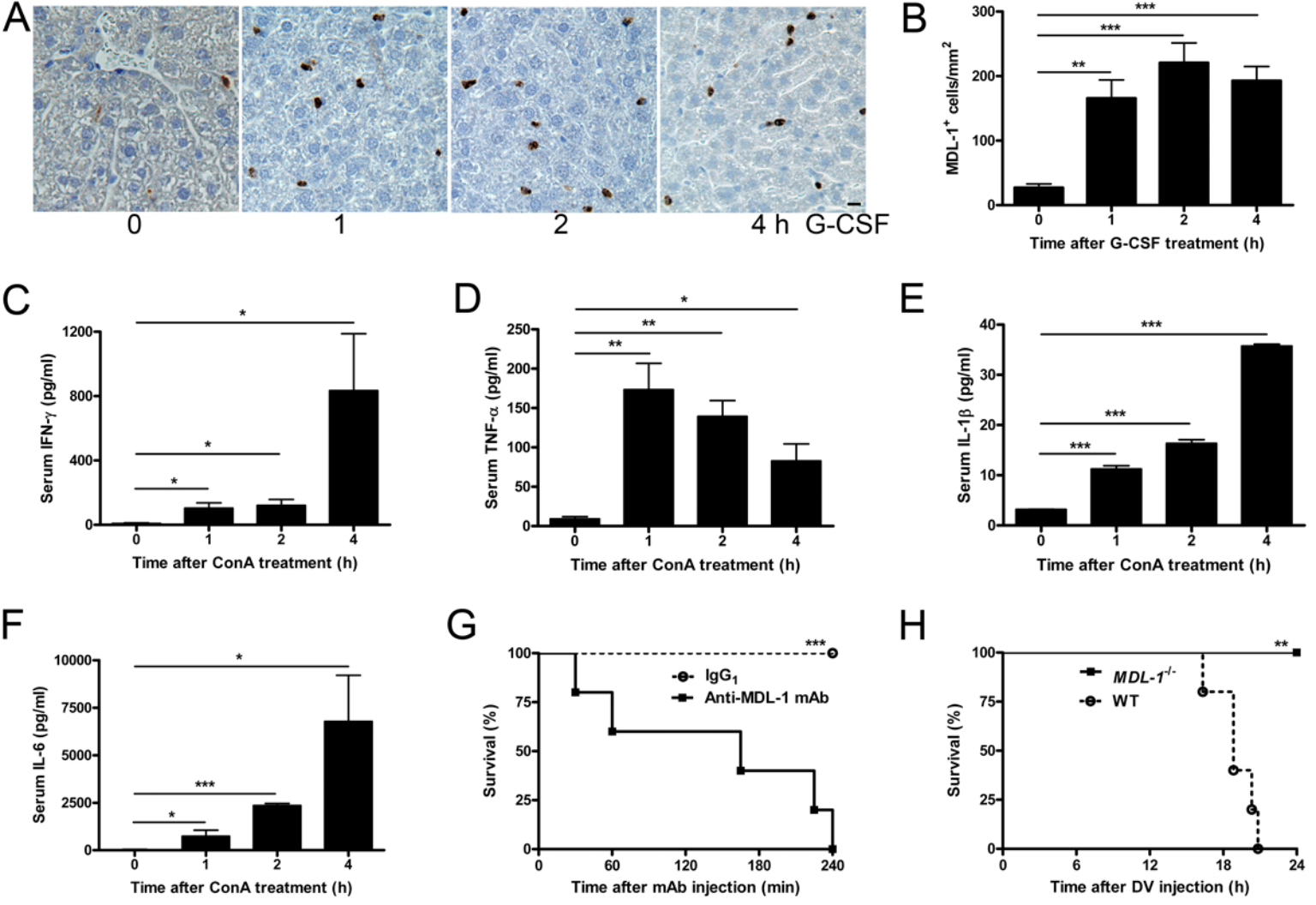

Supplemental Figure 2. G-CSF mobilizes hepatic infiltration of MDL-1⁺ cells, subsequent cytokine priming and MDL-1 activation cause lethal shock. **(A)** Mice were treated with G-CSF for indicated times (n=5) and liver sections were stained with anti-MDL-1 mAb. Scale bar: 10 μm. **(B)** Quantitation of MDL-1⁺ cells in (A). **P<0.01, ***P<0.001 compared to 0 h time point. **(C-F)** Sera were obtained from mice treated with ConA for indicated times (n=5). **(C)** IFN-γ, **(D)** TNF-α, **(E)** IL-1β, and **(F)** IL-6 levels in the sera were quantitated by Luminex. *P<0.05, **P<0.01, ***P<0.001 compared to naive sera. **(G)** Mice were treated with G-CSF, IFN-γ, TNF-α, IL-1β, IL-6, followed by anti-MDL-1 mAb (n=5) and survival was monitored. ***P<0.001 compared to IgG_1. **(H)** *MDL-1*$^{-/-}$ and WT mice were treated with G-CSF, IFN-γ, TNF-α, IL-1β, IL-6, followed by DV (n=5) and survival was monitored. **P<0.01 compared to WT.

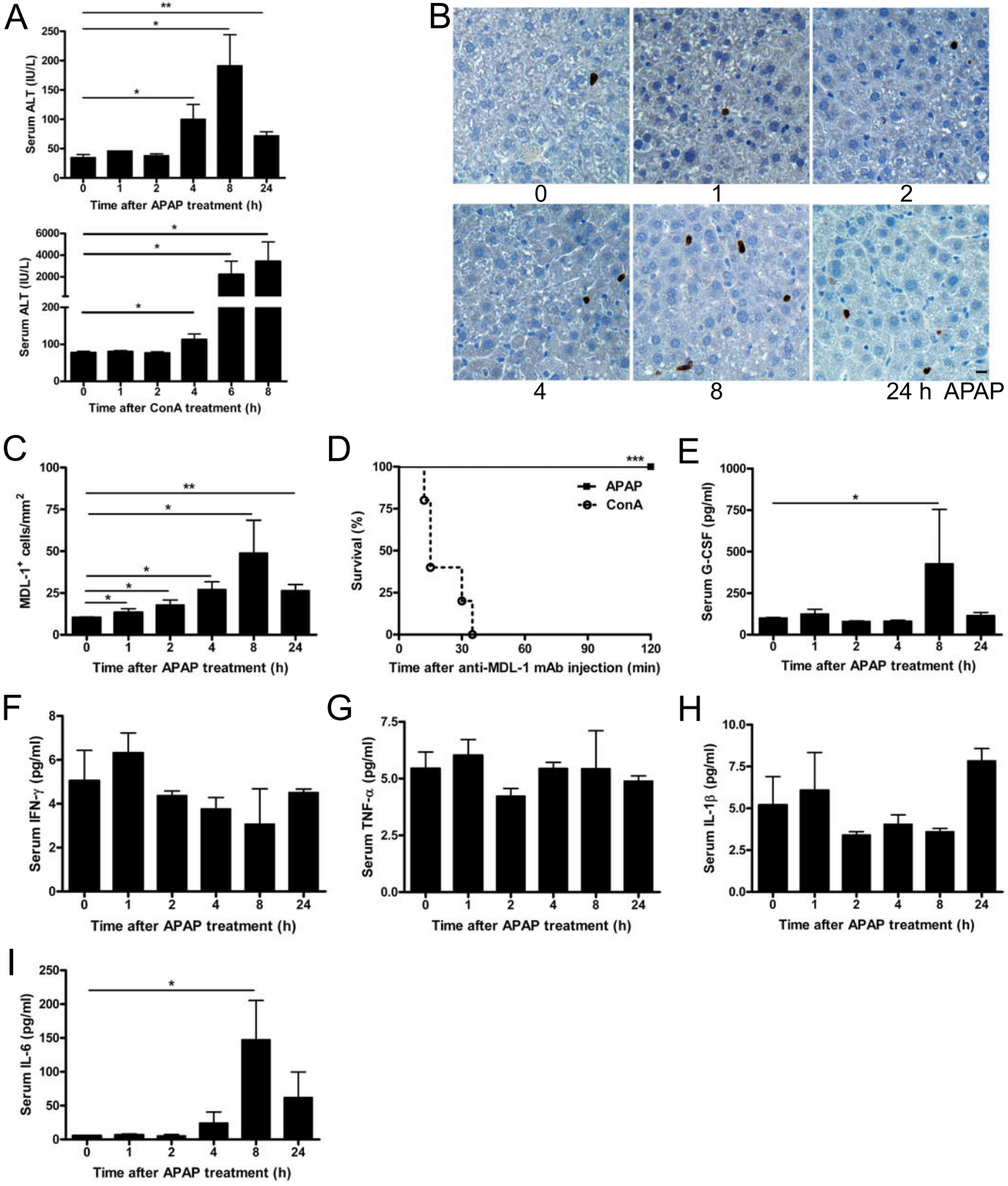

Supplemental Figure 3. APAP-induced liver injury weakly recruits MDL-1⁺ cells, and subsequent triggering of MDL-1 does not cause lethal shock. **(A)** C57BL/6 mice were treated with APAP (top) or ConA (bottom) for indicated times (n=5), sera were collected and serum ALT levels measured. *P<0.05, **P<0.01 compared to 0 h time point. **(B)** Liver sections from (A) were stained with anti-MDL-1 mAb. Scale bar: 10 μm. **(C)** Quantitation of MDL-1⁺ cells in (B). **(D)** Mice were treated with APAP for 8 h or ConA for 4 h followed by anti-MDL-1 mAb (n=5) and survival was monitored. ***P<0.001 compared to ConA treatment. **(E-I)** Serum taken from (A) was analyzed for **(E)** G-CSF, **(F)** IFN-γ, **(G)** TNF-α, **(H)** IL-1β, and **(I)** IL-6. *P<0.05 compared to 0 h time point.

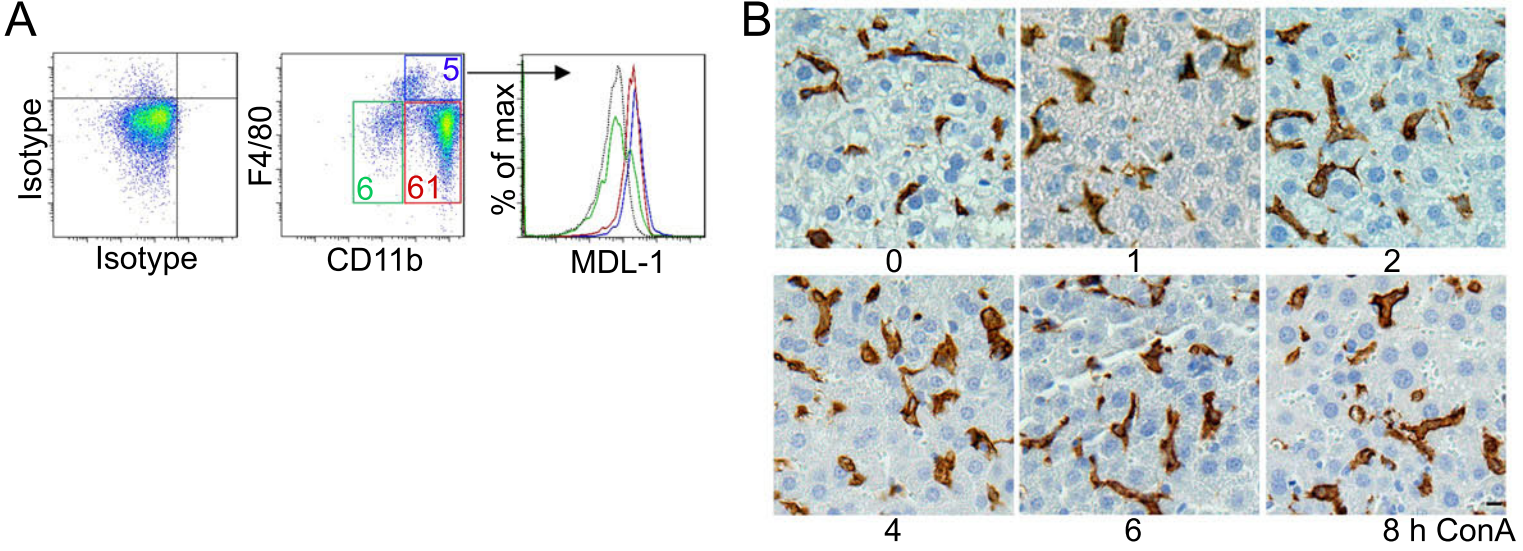

Supplemental Figure 4. MDL-1 is not expressed on macrophages. **(A)** Leukocytes isolated from livers of ConA-treated mice were purified using CD45 microbeads and analyzed by flow cytometry for expression of CD11b and F4/80 gated on $CD45^+$ cells. Background signal was established in the same population by staining with the matched isotype controls. Numbers indicate the percentage of $CD11b^+/F4/80^+$ (blue box), $CD11b^+/F4/80^-$ (red box), and $CD11b^-/F4/80^-$ (green box) cell population. Individual population was analyzed for MDL-1 expression (dotted line=isotype control). **(B)** Mice were treated with ConA for indicated times (n=5) and liver sections were stained with anti-F4/80 mAb. Scale bar: 10 μm.

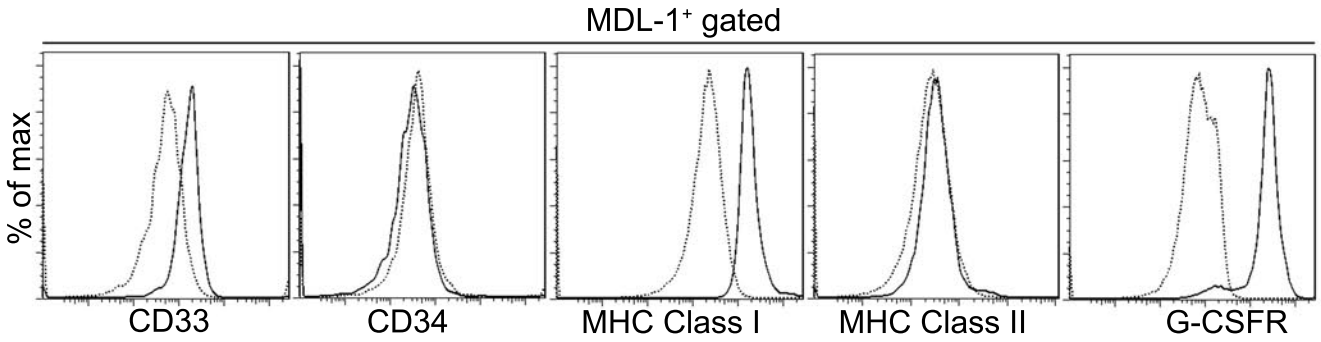

Supplemental Figure 5. Immunophenotyping of MDL-1$^+$ cells as CD33$^+$/CD34$^-$/MHC Class I$^+$/MHC Class II$^-$/G-CSFR$^+$ immature myeloid cells. Leukocytes isolated from livers of ConA-treated mice were purified using CD45 microbeads and analyzed by flow cytometry for expression of CD33, CD34, MHC Class I, MHC Class II and G-CSFR gated on MDL-1$^+$ cells (dotted line=isotype control).

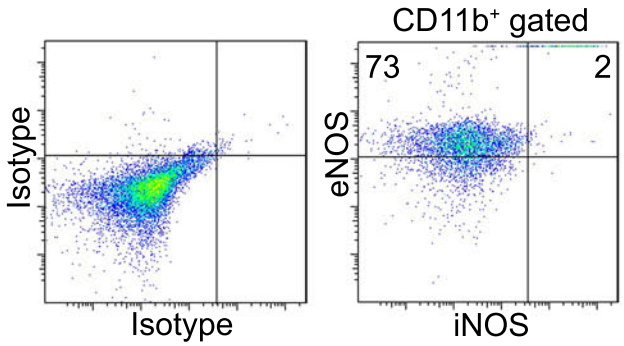

Supplemental Figure 6. iNOS is not expressed in immature myeloid cells. Leukocytes isolated from livers of ConA-treated mice were analyzed by flow cytometry for expression of eNOS and iNOS gated on CD11b$^+$ cells. Bakground signal was established in the same population by staining with the matched isotype controls (left panel).

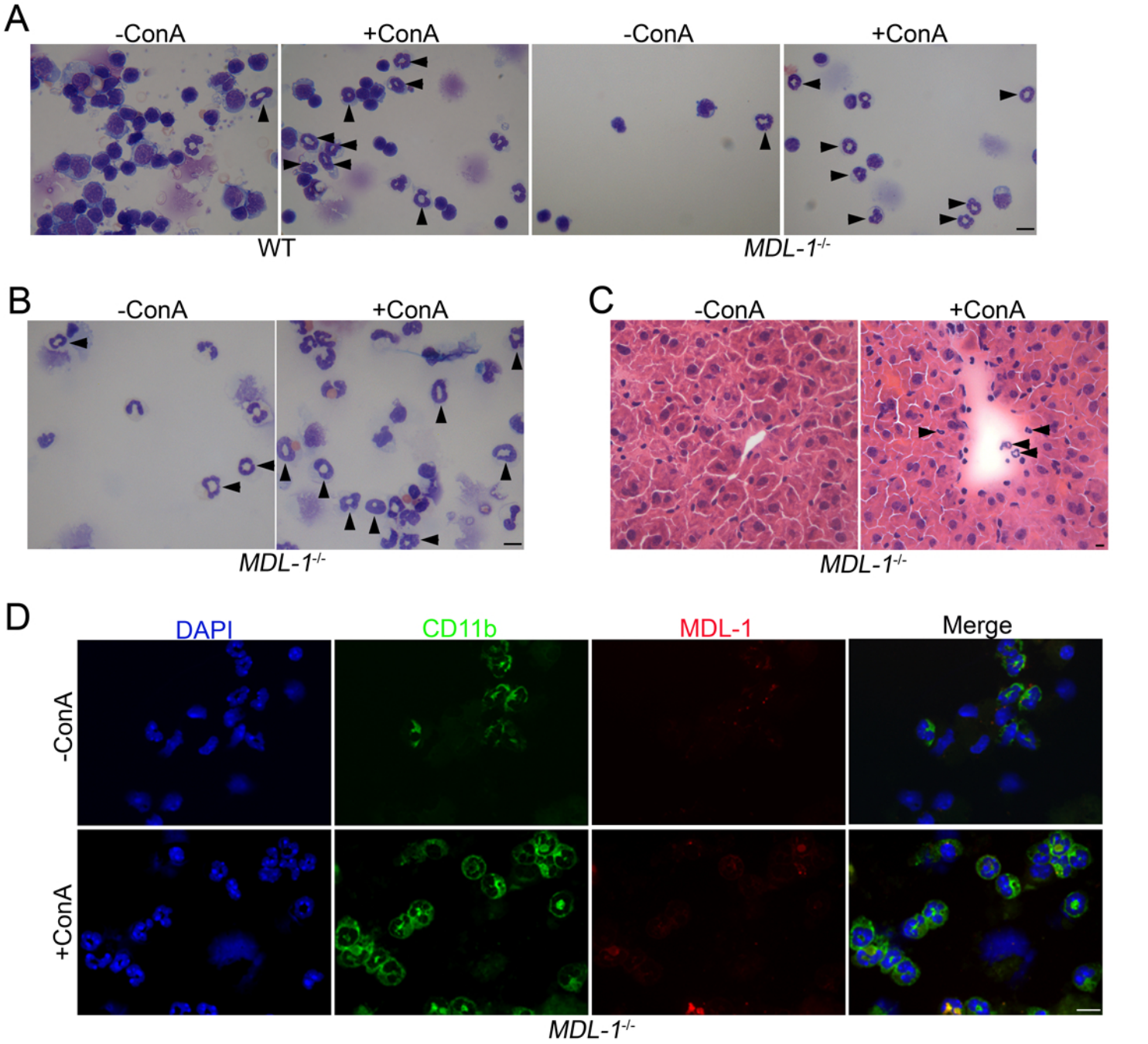

Supplemental Figure 7. ConA-induced infiltration of myeloid cells to blood and liver is MDL-1-independent. **(A)** Morphologic analysis of Diff-Quik stained cytospin preparations of Gr-1$^+$ cells isolated from blood of naive and ConA-treated WT and *MDL-1*$^{-/-}$ mice. Note the increased number of cells with ring-shaped nuclei (as indicated by arrows) by ConA treatment in both WT and MDL-1$^{-/-}$ mice. Scale bar: 10 μm. **(B)** Diff-Quik stained cytospin preparations of Gr-1$^+$ cells isolated from livers of naive and ConA-treated *MDL-1*$^{-/-}$ mice. Ring cells are indicated by arrows. Scale bar: 10 μm. **(C)** Representative micographs of H&E-stained liver sections from naive and ConA-treated *MDL-1*$^{-/-}$ mice. Ring cells are indicated by arrows. Scale bar: 10 μm. **(D)** Representative micrographs of immunostaining cytospin preparations of Gr-1$^+$ cells isolated from livers of naive (top panel) and ConA-treated (bottom panel) *MDL-1*$^{-/-}$ mice. Cells were stained with antibodies against CD11b (green) and MDL-1 (red). Nuclei were counterstained with DAPI (blue). Scale bar: 10 μm.

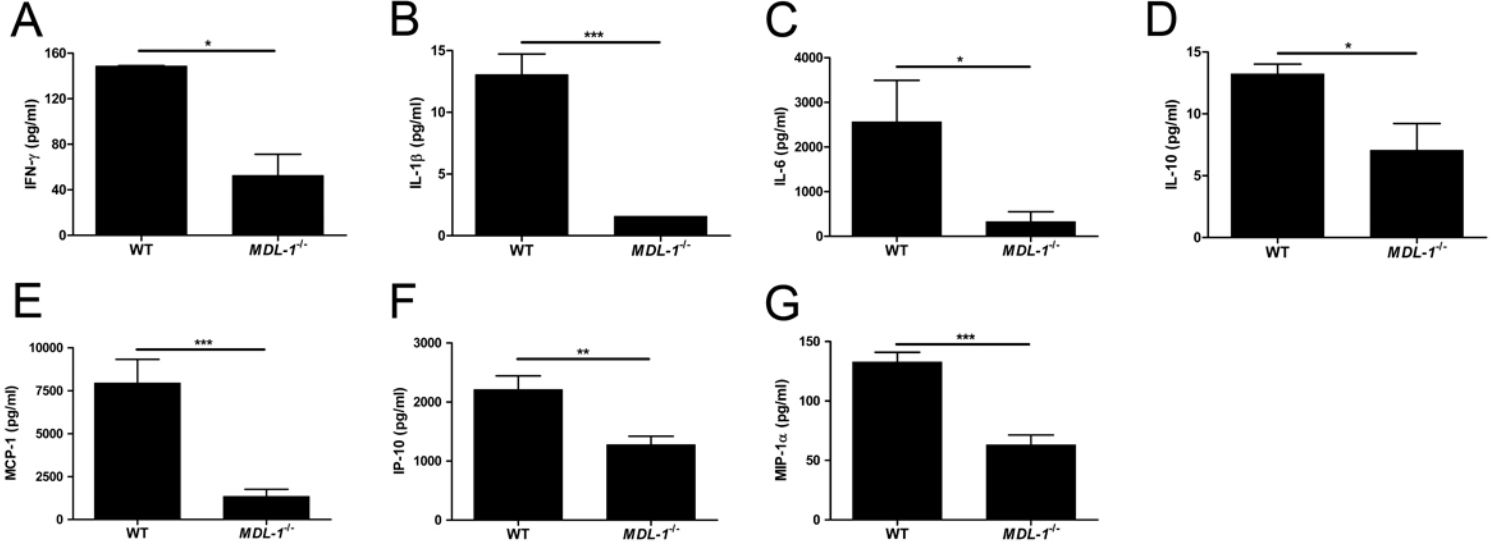

Supplemental Figure 8. MDL-1-triggered shock is associated with elevated serum levels of IFN-γ, IL-1β, IL-6, IL-10, MCP-1, IP-10 and MIP-1α. Serum was collected from WT and *MDL-1*$^{-/-}$ mice treated with ConA followed by anti-MDL-1 mAb (n=5). **(A)** IFN-γ, **(B)** IL-1β, **(C)** IL-6, **(D)** IL-10, **(E)** MCP-1, **(F)** IP-10, and **(G)** MIP-1α levels were quantitated by Luminex. *P<0.05, **P<0.01, ***P<0.001 compared to *MDL-1*$^{-/-}$.